Ab initio synthesis of the ozone ultraviolet continuum

Lawrence L. Lohr and A. J. Helman
Department of Chemistry, University of Michigan, Ann Arbor, Michigan 48109

(Received 23 September 1986; accepted 9 February 1987)

Potential energy surfaces for the ground and excited electronic states responsible for the Hartley continuum of ozone are used to obtain quadratic, cubic, and quartic force constants. Vibrational dependence of rotational constants to sixth order is calculated by perturbation theory. The spectroscopic constants enable computation of rovibronic energy levels. Overlap of ground state and excited state perturbed vibrational wave functions yield Franck–Condon factors. Electric dipole allowed rovibronic transitions are generated under the I^r representation. The entire set of results generate the ultraviolet absorption spectrum. It is shown that inclusion of anharmonic terms in the vibrational Hamiltonian has a small effect upon the final spectrum, whereas rotational broadening plays a greater role in achieving agreement with experiment.

INTRODUCTION

The ozone molecule continues to be of interest to theoretician and experimentalist.[1–7] This is due to its importance in atmospheric chemistry and physics, and its amenability to *ab initio* calculations.[8–10] It seemed to us that an improvement in theoretical band shapes is possible if several features normally disregarded for polyatomic systems were accounted for. These include transitions from discrete, Boltzmann-populated vibrational levels, anharmonic effects in a Franck–Condon spectral synthesis, and rotational fine structure.

In a recent article[11] the fact was expressed that certain features of absorption spectra are unique to polyatomic systems, including the vibrational structure of an electronic transition to a dissociative state.[12–14] This applies to ozone, in which the C_s dissociation pathway results in formation of diatomic oxygen which exists in a multitude of rovibronic states. Thus, our work may test such a concept on a system of interest. A word of caution in interpreting our results: It is completely nonempirical, making it difficult to compare with our calculations based upon fittings to spectral data. To our knowledge, this is the first such *ab initio* spectral synthesis for a polyatomic system.

Many studies have been concerned with the electronic states of ozone,[15–17] and a number of workers have performed studies of the ground-state potential energy surface.[17–21] The ground state of ozone has the experimental equilibrium geometry listed in Table I, while the excited $^1B_2$ state responsible for the Hartley continuum is believed to have a (C_{2v}) bond length of 2.655 bohr with a bond angle of 108°. This surface is inherently dissociative and correlates with the fragments $O_2(^1\Delta_g) + O(^1D)$.

Hay and Dunning have performed *ab initio* calculations for several electronic states of ozone.[15] Hay, Pack, Walker, and Heller generated spectra out of the (000) level using the Gaussian wave packet method.[22] Sheppard and Walker used the classical Wigner method to obtain ultraviolet spectra out of vibrationally excited ozone.[23] They employed both *ab initio* and empirically adapted surfaces, parametrized as outlined below.

Adler-Golden has also contributed an interesting study of ozone absorption.[24] In this work, a Franck–Condon spectral synthesis generated the ultraviolet continuum, over a wide temperature range. Agreement with experiment (CO_2 laser vibrationally excited ozone) is good, and a semiempirical expression is given for temperature-dependent ozone UV absorption.

This article presents the theory behind our generation of the spectrum. All spectroscopic constants are obtained in the process. The final section is a tabulation and discussion of our results.

THEORY

The current work proceeds from the *ab initio* results of Hay and Dunning, together with the parametrization of Sheppard and Walker.[15,22,23] Hence, we give details of this previous work first. Hay, Pack, Walker, and Heller performed the calculation of the *ab initio* potential energy surfaces which we employ. The GVB-PP (perfect-pairing) MCSCF technique was used in conjunction with a (3*s*2*p*1*d*) contracted Gaussian basis set for all surfaces. This was done over a grid of points described by $95° < \alpha < 135°$, $2.1 < r_1 < 10.0$ bohr, $1.9 < r_2 < 3.1$ bohr, with $r_2 \leqslant r_1$.

The authors[22,23] decided to fit their calculated surfaces

TABLE I. Calculated and experimental ozone geometries and vibrational frequencies.[a]

	$^1A_1$	Expt.[b]	$^1B_2$
r(bohr)	2.464	2.403	2.746
α(deg)	115.75	116.83	111.05
ω_1(cm^{-1})	1209.0	1134.90	822.8
	(1200.9)	(1103.1)	
ω_2(cm^{-1})	680.7	716.0	341.3
	(674.7)	(700.9)	
ω_3(cm^{-1})	1086.1	1089.2	1282.6*i*[c]
	(1038.7)	(1042.1)	

[a] Frequencies are the harmonic frequencies; the fundamentals ν_1, ν_2, and ν_3 are given in parentheses.
[b] Reference 5.
[c] Imaginary frequency.

 0021-9606/87/105329-08$02.10

to an analytic form, and chose that of Murrell, Sorbie, and Varandas,[19] with details given below. As the authors state[22] the accuracy of these $X(^1A_1)$ and $B(^1B_2)$ surfaces may be described by the number of points (N) and rms error (σ): $X(N=93), \sigma = (0.02\text{ eV}), B(N=93, \sigma = 0.06\text{ eV})$. Sheppard and Walker parametrized the *ab initio* surfaces calculated by Hay and Dunning as the sum of two-body and three-body terms:

$$V_{2B} = -D\sum_i e^{-\beta X_i}(1+\beta X_i+\gamma X_i^2+\delta X_i^3), \quad (1)$$

$$V_{3B} = [1-\tanh(\Gamma q_1)]\sum_{i=0}^{30} c_i\, p_i(q_1,q_2,q_3). \quad (2)$$

The term V_{2B} represents the potential contributed by the three pairs of oxygen atoms (given the form of an extended Morse potential), where $x_i = r_i - r_0$ for $i = 1,3$ is the displacement from the diatomic equilibrium separation r_0 and D is the dissociation energy in eV. The term V_{3B} represents the potential energy which cannot be accounted for by consideration of pair interactions and vanishes if any atom approaches infinite separation from the remaining two. Here Γ is a constant (for a given surface) which yields the correct asymptotic behavior, while q_1, q_2, and q_3 are external symmetry coordinates defined by

$$q_1 = \frac{1}{\sqrt{3}}(r_1 + r_1 + r_3 - R_0), \quad q_2 = \frac{1}{\sqrt{2}}(r_2 - r_3),$$

$$q_3 = \frac{\sqrt{2}}{\sqrt{3}} r_1 - \frac{1}{\sqrt{6}}(r_2 + r_3)$$

(R_0 is a constant for a given surface) and p_i are polynomials of the form $q_1^l b^m c^n$, where $b^2 = q_2^2 + q_3^2$, $c^3 = q_1(q_3^2 - 3q_2^2)$, and $0 \leqslant l + m + n \leqslant 7$. Values for the coefficients c_i are in the appendix of Sheppard and Walker's paper[23]; we have used the set based on *ab initio* diatomic curves.

Some key parameters for these surfaces are as follows. The vertical excitation energy from the $^1A_1$ equilibrium geometry to the $^1B_2$ surface is 5.36 eV, while the energy difference between their respective C_{2v} minima is 3.25 eV. In addition the $^1B_2$ state correlates with the fragments $O_2(^1\Delta_g) + O(^1D)$, lying 1.72 eV below the saddle point on the $^1B_2$ surface, or 1.53 eV above the $^1A_1$ ground state. There is a shallow minimum 0.3 eV lower still, or 1.23 eV above the ground state, along the C_s-dissociative pathway for the $^1B_2$ surface.

We devised a computer program to compute all derivatives to fourth order with respect to the internuclear separations r_1, r_2, and r_3 at any given geometry for both ground and excited ($^1B_2$) states. To determine harmonic frequencies and anharmonic constants we converted to normal coordinates Q_1, Q_2, and Q_3 for the three vibrational modes ν_1 (symmetrical stretch), ν_2 (angle bend), and ν_3 (asymmetrical stretch). This was done via the internal symmetry coordinates defined as

$$q_k = \frac{1}{\sqrt{2}}(r_2 + r_3), \quad q_l = r_2(\alpha - \alpha_e),$$

$$q_m = \frac{1}{\sqrt{2}}(r_2 - r_3).$$

Here note that r_2 and r_3 are the bonded internuclear distances, while r_1 is the nonbonded distance. Such a transformation of derivatives through fourth order was nontrivial, and involved the evaluation of dozens of terms based on the Jacobian $\partial(q_k, q_l, q_m)/\partial(r_1,r_2,r_3)$. The calculations were performed by the program. The L matrix which converts symmetry adapted to normal coordinates was found by standard GF matrix formalism, obtaining enroute the zeta-matrix elements for both electronic states. Let z be the C_2 axis and x be perpendicular to the molecular plane. Using this choice of axes (known simply as the I^r representation), only the ζ^y 3×3 matrix is nonzero, as

$$\zeta^y = \begin{pmatrix} 0 & 0 & \zeta^y_{13} \\ 0 & 0 & \zeta^y_{23} \\ -\zeta^y_{13} & -\zeta^y_{23} & 0 \end{pmatrix}. \quad (3)$$

Having thus arrived at a listing of all force constants to fourth order, one seeks to determine how the vibrational wave functions, being harmonic oscillator (HO) functions in zeroth order, are perturbed by the presence of six cubic force constants and six quartic constants. Using first order perturbation theory one writes

$$\psi^{(1)}_{ijk} = \psi^{(0)}_{ijk} + \sum_{\{i',j',k'\neq i,j,k\}} \frac{\langle\psi^{(0)}_{ijk}|\mathscr{H}^P|\psi^{(0)}_{i'j'k'}\rangle}{(E^{(0)}_{ijk} - E^{(0)}_{i'j'k'})}\psi^{(0)}_{i'j'k'}, \quad (4)$$

where $\psi^{(0)}_{ijk}$ is a triple product of HO wave functions $\psi^{(0)}_i\,\psi^{(0)}_j\,\psi^{(0)}_k$, $\mathscr{H}^P$ is the anharmonic Hamiltonian operator, and $\psi^{(1)}_{ijk}$ is the corrected function. Such an algorithm was devised for the 20 lowest-lying states of $^1A_1$ zone, plus the 555 lowest lying states of $^1B_2$ ozone; for the latter (4) is replaced by a sum of double products as we are considering only the nondissociative modes Q_1 and Q_2 at this stage. The number of $^1B_2$ vibrational states was based upon considerations of the Los Alamos surface, and reflects the semiclassical nature of the wave function amplitude for large values of v_1' and v_2'. In fact, a subsidiary program was needed to calculate all Hermite polynomials to order 50. The evaluation of Eq. (4) above was performed numerically using the Romberg method to derive Cotes sums over a grid of points broad enough that the exponential factor in $H_n(x)$ had decayed to at least e^{-8}, thereby ensuring sufficient coverage for the integration procedure.[25] This was a triple integration; the three-dimensional $[q_1, q_2, q_3]$ surface was summed over with a set of approximately one-third million points. A comparison of the vibrational energies obtained using this perturbation approach to experiment and to energies obtained by others using variational methods is given in the next section.

The perturbed vibrational wave functions are first used to find the vibrational dependence of the three rotational constants B_x, B_y, B_z. Here

$$\frac{1}{r_{ijk}} = \left\langle\psi^{(1)}_{ijk}\left|\frac{1}{r}\right|\psi^{(1)}_{ijk}\right\rangle \quad (5)$$

and

$$\frac{1}{\alpha_{ijk}} = \left\langle\psi^{(1)}_{ijk}\left|\frac{1}{\alpha}\right|\psi^{(1)}_{ijk}\right\rangle, \quad (6)$$

where $\psi^{(1)}_{ijk}$ is the corrected (perturbed) wave function for either electronic state.

Care must be exercised in recovering r_i from this expression, as we are in normal coordinates. The success of the above was evident in a smooth, quasilinear variation of the rotational constants with increasing vibrational quantum number, in accord with the experimental result that

$$B_k^v = B_k^{eq} - \sum_k \alpha_k^\beta (v + \tfrac{1}{2}). \tag{7}$$

Here v is the vibrational quantum number and $k = x, y, z$ (I^r rep.).

Using standard formulas[26] one easily computes the vibrational level energies in cm^{-1}, given the harmonic frequencies and anharmonic constants. Any levels closer than 50 cm^{-1} were then recorrected due to Darling–Dennison resonance, employing γ calculated from the data. In truth such a resonance exists between the (200) and (002) levels of ground state ozone.[27]

Having found the vibrational band origins we calculate the higher order rotational constants starting with the B_k above. The theory employed is that of contact transformations,[28] leading to the result that the vibrational–rotational Hamiltonian is just $H = \Sigma_{m,n} H_{mn}$, where m refers to the degree of the vibrational operators and n to the degree of the components of the angular momentum operator **J**.

Considering more specifically the pure rotational Hamiltonian, using the notation of Watson[29] one has

$$\mathscr{H}^{rot} = \sum_{p,q,r=0} h_{pqr} (J_x^p J_y^q J_z^r + J_z^r J_y^q J_x^p), \tag{8}$$

h_{pqr} being a constant. The expression is written as is because it should be Hermitian. We wish to apply a unitary transformation to the given Hamiltonian in such a fashion that its general form remains the same, yet with new coefficients. We write $H = U^{-1}HU$, where U is one such unitary transformation. Selecting the form $U = e^{iS}$ is convenient, as it requires only that S be Hermitian. We may separate S and thereby factor U as

$$U = e^{iS_1} \cdot e^{iS_3} \cdot e^{iS_5} \cdots, \tag{9}$$

where S has only terms such that $p + q + r = n$. The important result is that for any given order of the rotational Hamiltonian, the terms off-diagonal are removed to the next higher order, allowing for the determination of formulas for the quartic, sextic, etc., constants.

With this background, the quartic and sextic centrifugal distortion coefficients are determined as follows. Inertial defined as $a_k^{\alpha\beta} = (\partial I_{\alpha\beta}/\partial Q_k)_e$ (a.u.) are used to find rotational derivatives, defined as

$$B_k^{\alpha\beta} = B_k^{\beta\alpha} = -(\hbar^3/2h^{3/2}c^{3/2}\omega^{1/2})(a_k^{\alpha\beta}/I_\alpha I_\beta). \tag{10}$$

Here $I_{\alpha\beta}$ is an element of the inertia tensor and Q_k is a normal mode. Due to symmetry considerations it turns out that there are only six nonzero $B_k^{\alpha\beta}$. Finally one has $\tau_{\alpha\beta\gamma\delta} = -2\Sigma_k B_k^{\alpha\beta} B_k^{\gamma\delta}/\omega_k$ for the quartic centrifugal distortion coefficients. One converts these to "primed" coefficients by $\tau'_{aaaa} = \tau_{aaaa}$, $\tau'_{aa\beta\beta} = \tau_{aa\beta\beta} + 2\tau_{\alpha\beta\alpha\beta}$, and uses these to find the empirical constants Δ_J, Δ_{JK}, Δ_J, etc., as linear combinations of the $\tau'_{\alpha\beta\gamma\delta}$. Again the I^r representation is used. The appropriate expressions are given in the appendix of Kivelson and Wilson's paper.[30]

The computation of rotational energy levels is made simpler by initial transformation of the rotational Hamiltonian to cylindrical tensor form[28]:

$$\mathscr{H}^{rot} = \mathscr{H}_{02} + \mathscr{H}_{04} + \mathscr{H}_{06} = \{B_{200}\tilde{J}^2 + B_{020}J_z^2 + T_{400}(\tilde{J}^2)^2 + T_{220}\tilde{J}^2J_z^2 + T_{040}J_z^4 + \Phi_{600}(\tilde{J}^2)^3$$
$$+ \Phi_{420}(\tilde{J}^2)^2J_z^2 + \Phi_{240}\tilde{J}^2J_z^4 + \Phi_{060}J_z^6\} + \tfrac{1}{2}[(B_{002} + T_{202}\tilde{J}^2 + T_{022}J_z^2 + \Phi_{402}(\tilde{J}^2)^2 + \Phi_{222}\tilde{J}^2J_z^2 + \Phi_{042}J_z^4),(\tilde{J}_+^2$$
$$+ \tilde{J}_-^2)]_+ + \tfrac{1}{2}[(T_{004} + \Phi_{204}\tilde{J}^2 + \Phi_{024}J_z^2),(\tilde{J}_+^4 + \tilde{J}_-^4)] + \Phi_{006}(\tilde{J}_+^6 + \tilde{J}_-^6), \tag{11}$$

where $[\tilde{P},\tilde{Q}]_+ = \tilde{P}\tilde{Q} + \tilde{Q}\tilde{P}$ (anticommutator), and $\tilde{J}_\pm = \tilde{J}_x \pm i\tilde{J}_y$. Due to the presence of arbitrary parameters in Eq. (11), certain assumptions are usually made. In the "A" reduction, one sets $T_{004} = \Phi_{204} = \Phi_{024} = \Phi_{006} = 0$. One then obtains a form for the Hamiltonian in which the diagonal elements are given by[28]

$$E_{KK} = \langle J,K|\mathscr{H}_{rot}^{(A)}|J,K\rangle = \tfrac{1}{2}[B_x + B_y]J(J+1) + \{B_z - \tfrac{1}{2}(B_x + B_y)\}K^2 - \Delta_J J^2(J+1)^2$$
$$- \Delta_{JK}J(J+1)K^2 - \Delta_K K^4 + \Phi_J J^3(J+1)^3 + \Phi_{JK}J^2(J+1)^2K^2 + \Phi_{KJ}J(J+1)K^4 + \Phi_K K^6 \tag{12}$$

and off-diagonal elements are simply[28]

$$E_{K,K\pm2} = \langle J,K\pm2|\mathscr{H}_{rot}^{(A)}|J,K\rangle = \{\tfrac{1}{4}[B_x - B_y] - \delta_J J(J+1) - \tfrac{1}{2}\delta_K[(K\pm2)^2 + K^2] + \phi_J J^2(J+1)^2 + \tfrac{1}{2}\phi_{JK}$$
$$\times J(J+1)[(K\pm2)^2 + K^2] + \tfrac{1}{2}\phi_K[(K\pm2)^4 + K^4]\} \times \{[J(J+1)$$
$$- K(K\pm1)][J(J+1) - K(K\pm1)(K\pm2)]\}^{1/2}. \tag{13}$$

Here the superscript "A" refers to the A reduction, while the relations between the coefficients in Eqs. (12) and (13) to those in Eq. (11) have been given.[28]

Recall that ozone, with an asymmetry parameter $\kappa = -0.968$, is a nearly prolate asymmetric top, for which there are $2J + 1$ values of K_{-1} ranging from $-J$ to J. Thus one must diagonalize a set of matrices, J_{max} in number, of increasing size up to $(2J_{max} + 1) \times (2J_{max} + 1)$. Fortunately, each J block may be factored into a K_{-1}-even and a K_{-1}-odd subblock.[31] Figure 1 reveals that these subblocks are in simple tridiagonal form, and hence the complete eigensystem is solved by any subroutine which diagonalizes tridiagonal real, symmetric (Hermitian) matrices. In the actual program, the diagonal elements are components of a vector of dimension $\Sigma_{J=0}^{J_m}(2J+1)$,[2] and the off-diagonal elements are placed in a similar vector of dimension J_{max}^2. The eigen-

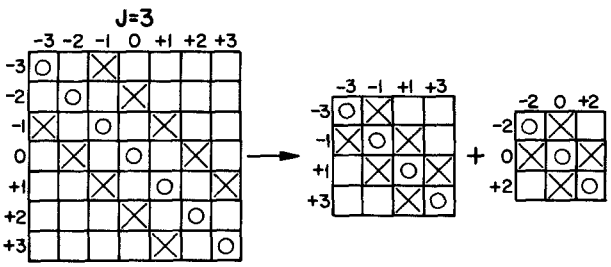

FIG. 1. Factoring of $J = 3$ matrix into K_{-1} odd and even subblocks. Circles are diagonal elements, crosses off-diagonal.

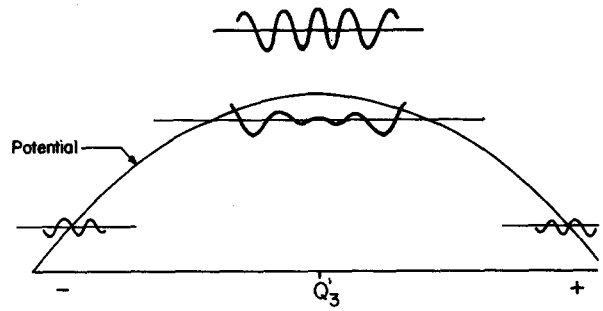

FIG. 3. Wave function amplitude for the asymmetric stretch mode of $^1B_2$ ozone.

values are returned to the original vector and added to the vibrational energies.

For $^{16}O_3$ the only allowed rovibronic levels are those of A_1 and A_2 permutation-inversion (PI) symmetry, where the PI group is isomorphous with the point group C_{2v}. Figure 2 shows the construction of these from electronic, vibrational, and rotational factors as well as the allowed electric dipole transitions, namely A_1 to A_2, where the laboratory-frame dipole operator μ_Z transforms as the A_2 representation of the PI group. We also note here that the Coriolis interaction within each electronic manifold involves the mixing of a_1 vibrational levels (even number of quanta in the b_2 asymmetric stretching mode) with b_2 vibrational levels (odd number of quanta in this mode).

Consider the determination of Franck–Condon factors for the $^1B_2 \leftarrow {}^1A_1$ transition. As one wishes to make explicit the anharmonic force fields effect upon band structure, one cannot use standard formulas for the overlap of HO functions.[32] One must express the excited-state normal coordinates in terms of the ground-state normal coordinates, or vice versa, in order to evaluate the overlap integrals. Using matrix algebra one has

$$Q'' = L''A''(A'^{-1}K'Q' + R) \qquad (14)$$

for conversion from excited state (Q') to ground-state (Q'') coordinates. The K″ is inverse to the excited L′ matrix, A converts internuclear separation coordinates to symmetry coordinates, and R is the displacement vector between the ground-state equilibrium geometry and the quasiequilibrium geometry of the excited state. Thus, all excited state functions are expressed in terms of ground-state normal coordinates, and the overlap integrals are readily evaluated.

A problem persists for the evaluation of the factor $\langle \psi_{v_3'} | \psi_{v_3} \rangle$, as the asymmetric stretch mode for the excited state, represented by $\psi_{v_3'}$, is essentially a perturbed, inverted

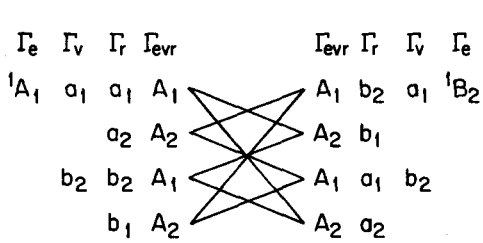

FIG. 2. Pattern of electronic, vibrational, and rotational components of rovibronic states connected by the electric dipole operator μ_Z which transforms as the A_2 irreducible representation of the permutation-inversion group for $^{16}O_3$.

harmonic oscillator. The Schrödinger equation for a harmonic barrier may be brought into the simplified form $z'' + (ax^2 + b)z = 0$. Assuming a power-series solution of the form $z = \Sigma_{n=0}^{\infty} c_n x^n$ one obtains two independent solutions which are essentially the parabolic cylinder functions. The three-term recursion formula we have derived is $c_{n+4} = -(ac_n + bc_{n+2})/[(n+3)(n+4)]$. The power series obtained is convergent for reasonable values of coordinate x (Q_3' in a.u.) only upon going to the 50th or 60th power. However, our solutions do give the physically reasonable result that the wave function behaves as indicated in Fig. 3, for various heights above and below the top of the barrier. It turned out that the greatest amount of overlap with ground state wave functions occurs slightly above the barrier top, corresponding to a positive kinetic energy needed to form fragments.

The final program receives input from all prior programs (vibrational energies, rotational levels, overlap integrals, etc.) and generates an absorption spectrum assuming a constant electronic factor and a Boltzmann population of all ground rovibronic states. The assumption of a constant factor for the overlap of electronic wave functions was for the sake of computational tractability. In addition Hay and Dunning[15] have calculated a transition dipole moment for the $^1B_2 \leftarrow {}^1A_1$ transition, and this is the factor used in our work. Note that anharmonic effects are made manifest in at least two ways: spacing of vibrational levels and magnitude of overlap integrals. The output is stored in 1 cm^{-1} wide energy bins across the spectral region 0–50 000 cm^{-1}.

RESULTS AND DISCUSSION

Table I lists harmonic frequencies for the two electronic states $^1A_1$ and $^1B_2$ together with vibrational fundamentals for the state $^1A_1$. Also given are the equilibrium geometries for both electronic states, obtained by setting all first partial derivatives equal to zero for the surfaces employed. These values are accurate to 0.001 bohr and 0.05° for the bond distance and bond angle, respectively. Comparison of the ground-state equilibrium geometry with the experimental geometry indicates that the ground surface is quite accurate for our purposes. However, the authors[22] state that the rms error for their excited state is three times greater than for the ground state. Thus, although the ground state $\omega_1, \omega_2, \omega_3$ are roughly within $\pm 6\%$ of experiment (with ω_3 being fortuitously close and with ω_1 being too large and in the worst

TABLE II. Calculated and experimental quadratic, cubic, and quartic force constants.[a,b]

	$^1A_1$	Expt.[c]	$^1B_2$
f_r	6.02	6.163	8.61
f_{rr}	1.47	1.602	5.74
f_α	1.32	1.300	0.40
$f_{r\alpha}$	0.36	0.402	0.26
k_{111} (cm^{-1})	−49.18	−48.1	−27.62
k_{222} (cm^{-1})	−19.24	−19.2	−8.47
k_{112} (cm^{-1})	−54.49	−29.7	−18.02
k_{122} (cm^{-1})	−32.96	−25.5	−6.55
k_{133} (cm^{-1})	−225.47	−225.8	+91.63
k_{233} (cm^{-1})	−86.22	−59.3	+14.77
k_{1111} (cm^{-1})	+10.51	+2.2	+3.69
k_{2222} (cm^{-1})	+3.05	+0.6	−2.06
k_{3333} (cm^{-1})	+4.51	+6.7	−5.65
k_{1122} (cm^{-1})	+14.32	−1.8	+4.81
k_{1133} (cm^{-1})	+28.10	+28.3	−16.84
k_{2233} (cm^{-1})	+22.31	−5.9	−9.93

[a] The energy of $^1B_2$ ozone has been expanded about its calculated quasiequilibrium as listed in Table I.
[b] Quadratic force constants in mdyn/Å.
[c] Reference 5.

agreement), the values for the excited state may be of less certainty.

Listed in Table II are calculated quadratic, cubic, and quartic force constants, plus the ground-state values obtained by the usual spectroscopic fitting procedure. The calculated values for the ground-state cubic constants correctly predict both the relative size of these constants, and in most cases are accurate within ± 15%. Such agreement is also predicted for the excited state cubic constants, except for the relative crudity of this surface. In contrast the ground-state quartic force constants agree only in order of magnitude with spectroscopic data, and sometimes even the wrong sign is predicted. However, the large value of k_{1133} is still apparent in the *ab initio* data, as well as some remarkably close agreements for some of the other constants.

Figure 4 displays the effect of anharmonic terms upon

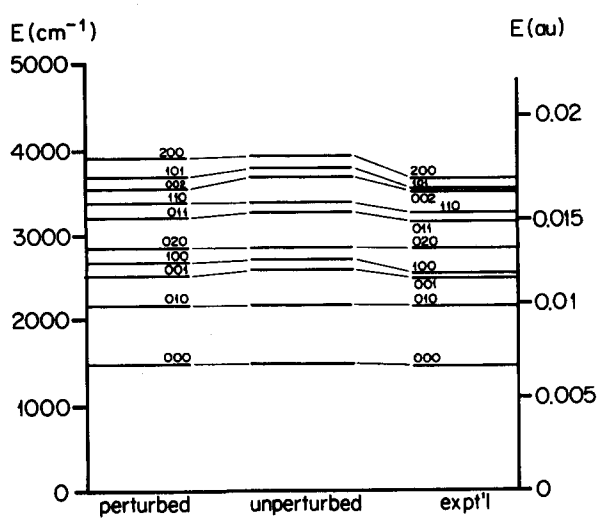

FIG. 4. Effect of anharmonicity upon ozone band origins. Energies are relative to potential minimum. Experimental energies from Ref. 5 except for the (020) state from Ref. 3(b).

TABLE III. Calculated and experimental rotational constants[a] for the (000) levels.

	$^1A_1$	Expt.[b]	$^1B_2$
B_x	0.3820	0.394 751 810	0.3246
B_y	3.2885	3.553 666 33	2.3368
B_z	0.4322	0.445 283 212	0.3770

[a] In cm^{-1}.
[b] Reference 33.

calculated vibrational levels for the ground state. The results of our perturbation treatment bring the levels into closer agreement with experiment[3(b),5] than otherwise. Overall, the level of agreement is satisfactory, although with the computed fundamental ν_1 being 97 cm^{-1} too large (Table I), the overtone (200) and the combinations (110) and (101) are also too large, by 213, 90, and 88 cm^{-1}, respectively. The overtones (020) and (002) are 44 and 10 cm^{-1} too low, respectively, while the combination (011) is only 8 cm^{-1} too low. The recent variational calculations[21(b)] of Adler-Gorden *et al.* using a CASSCF/DZP *ab initio* surface yielded fundamentals, overtones, and combinations of comparable agreement with experiment, but with ν_1 being 53 cm^{-1} too low rather than too large and with ν_3 being 114 cm^{-1} too low rather than being essentially correct (our error is only 4 cm^{-1}; Table I). However, the vibrational levels they obtained variationally using an empirically adjusted multidimensional perturbed Morse oscillator surface are better than ours, with deviations from experiment of 5 cm^{-1} or less, or somewhat better than the agreement obtained earlier by Carter *et al.*[6(a)] also using a variational method and an empirically adjusted potential energy surface. We conclude that our combined use of an *ab initio* surface perturbation theory, and numerical integration to obtain the perturbed vibrational energies and wave functions is generally satisfactory for our semiquantitative needs as input to the UV band shape calculation, although not satisfactory for reproducing precise details of the ground-state IR spectrum.

The rotational constants B_x, B_y, B_z for the (000) level of both the $^1A_1$ and $^1B_2$ states are listed in Table III. Agreement[33] is good.

Due to the many means of defining quartic centrifugal distortion constants, care should be exercised in comparing published values. This is because of different axis labeling

TABLE IV. Calculated and experimental quartic centrifugal distortion coefficients.[a]

	$^1A_1$	Expt.[b]	$^1B_2$
Δ_J	7.84×10^{-7}	$4.542\,716\,76\times10^{-7}$	9.24×10^{-7}
Δ_{JK}	-2.31×10^{-5}	$-1.846\,052\,22\times10^{-6}$	6.69×10^{-6}
Δ_K	1.76×10^{-4}	$2.116\,612\,13\times10^{-4}$	2.88×10^{-4}
δ_J	9.87×10^{-8}	$6.679\,660\,80\times10^{-7}$	1.01×10^{-8}
δ_K	4.34×10^{-5}	$3.233\,080\,15\times10^{-6}$	2.35×10^{-6}
R_5	-2.10×10^{-5}	...	-1.46×10^{-5}

[a] In cm^{-1}.
[b] Reference 33.

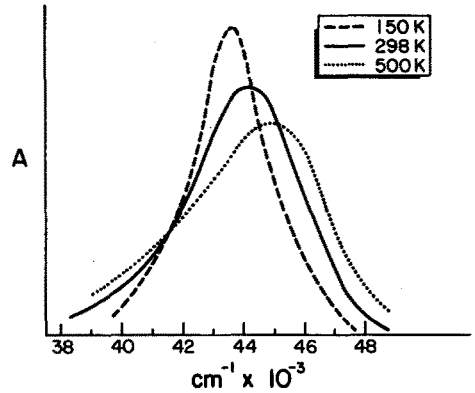

FIG. 5. Classical band shape at three temperatures.

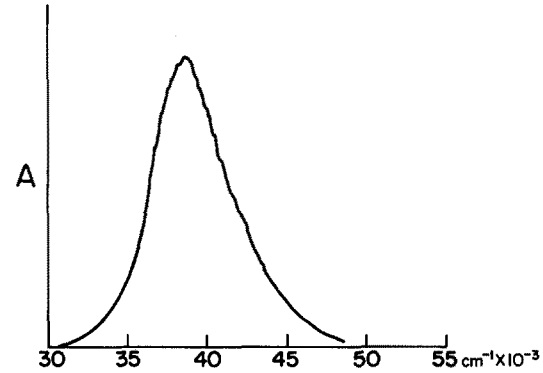

FIG. 7. Synthesized absorption from the (000) level with $T_{rot} = 298$ K. This spectrum as well as those in Figs. 9 and 10 have been red shifted by 4620 cm^{-1}.

schemes and because some prefer to report in the $\tau_{\alpha\beta\gamma\delta}$ themselves while others report in their experimentally determined linear combinations. In Table IV we adopt the latter usage, under the I^r representation and using the Δ_J, etc. as defined in the appendix of Watson's paper.[29] Direct comparison of this data to results obtained by the usual fitting procedure would be inappropriate and grossly underestimate the value of our calculations. A better set of *ab initio* quartic centrifugal distortion constants for ozone has recently been obtained by us[34] at the HF/6-31G** and MCSCF levels using a new method[35] employing analytical *ab initio* gradients.

A classical band shape calculation[36,37] taking no account of vibrational structure is shown by Fig. 5. There is a temperature shift of the absorption maximum. This shift in frequency is positive with rising temperature, starting at 43 220 cm^{-1} at 0 K and at the three temperatures indicated represent a shift of 650, 1180, and 1980 cm^{-1}. In addition the bandwidth at half-height agrees with the trend that the classical bandwidth rises with temperature, and equals the quantum-mechanical bandwidth at $T = \infty$. (For a one-dimensional HO the ratio[36] of classical to quantum bandwidths is $[\tanh x/x]^{1/2}$, where $x = h\nu/2kT$.) Note also the skewness of the spectra (third moment), a result of the nonidenticality of the ground- and excited-state vibrational frequencies.[36]

Figures 6–10 illustrate several calculated spectra plus the experimental data.[38] The energy scale has been red shifted 4620 cm^{-1} for the synthesized spectra, and an arbitrary set of intensity units has been affixed to all diagrams. This ensures ease of comparison. All spectra shown were run for $T = 298$ K. The main features are shown by comparison of the experimental spectrum (Fig. 6) to the calculated spectrum for excitation from the (000) level alone (Fig. 7). Not only has the proper overall band shape been realized, but also the effect of excitation into a vibrationally excited purely dissociative state is evident in the fine structure of the continuum. The numerical data reveals a series of progressions. There is a basic periodicity of some 820 cm^{-1} and one of 340 cm^{-1}. As overlap of zeroth order HO functions is appreciable only for low values of vibrational quantum number, Fig. 8 suffices as a rough guide to the origin of the alternating 140 and 200 cm^{-1} periodicity in the synthesized spectra. The region from ν_1' to $2\nu_1'$ is emphasized, although any other portion may have served by substitution of $(n+1)\nu_1'$ and $(n+2)\nu_1'$ for ν_1' and $2\nu_1'$, respectively. The experimental spectrum exhibits a similar structure, although the exact periodicity of the progressions await publication. Rotational broadening is seen in the smooth transition from one vibrational peak to the next. It is intriguing that such structure should be present in excitation to a dissociative state, illustrating the presence of diffuse vibrational structure in continuous UV spectra as treated by Pack.[11] The Huggins system of bands is believed due to a $^1B_2 \leftarrow {}^1A_1$ transition into a shallow well in the $^1B_2$ surface, allowing for sharpened vibrational structure.[39] Our work is in agreement with this assignment, with a minimum at $r_2 = 3.585\ a_0$, $r_3 = 2.295\ a_0$, $\alpha = 74°$ being located within the analytically fitted surface we employed.[15,22] Note this is a C_{2v} structure with an acute bond angle, in the excited state.

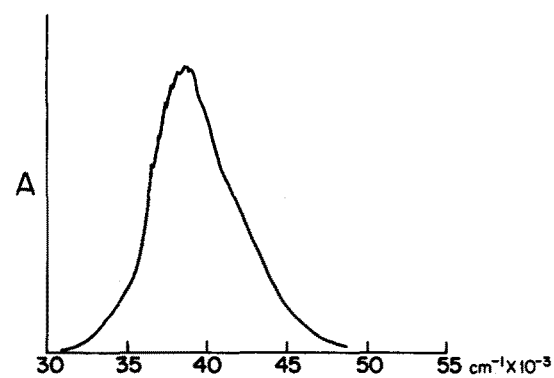

FIG. 6. Experimental absorption spectrum from Ref. 38 at 300 K.

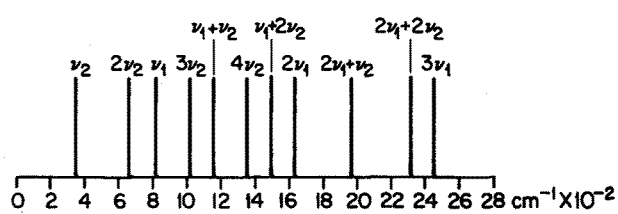

FIG. 8. Explanation for progressions in synthesized UV spectrum.

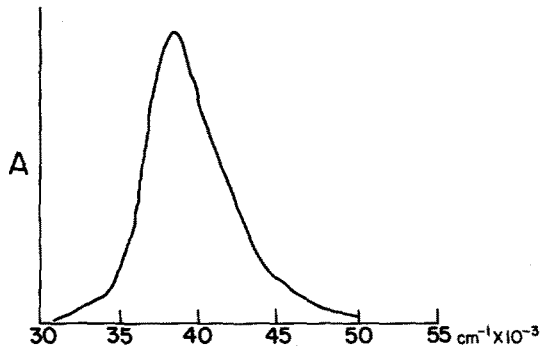

FIG. 9. Synthesized absorption from the 20 lowest bands of $X\,^1A_1$. $T_{vib} = T_{rot} = 298$ K.

When the calculation was performed at the theoretical 0 K for excitation out of the (000) level, only the $J = 0$ level is populated and one expects to see a diminution in the continuity of the progressions noted in Fig. 7. This is due to the absence of rotational broadening, and was "observed" for this computer "experiment" at absolute zero.

The suppression of rotational effects ($T_{rot} = 0$, $T_{vib} = 298$ K) diminished the quality of our calculated spectrum, as the rotational broadening disappears and we were unable to reproduce the experimental spectrum. Thus, it is likely that the effect of rotational broadening should be included if one seeks an improvement in the quality of calculated spectra. Comparison of Figs. 7 and 9 shows the effect of considering excitation from the 20 lowest vibrational levels of ground-state ozone. At 298 K these account for over 99% of the population. The progressions of Fig. 7 are somewhat damped out in Fig. 9, probably due to an averaging process from considering twenty rather than a single band. Again, the agreement with experiment is good.

Figure 10 shows the effect of including cross terms in the exited state vibrational wave functions, in effect the anharmonicity of the excited state. Comparison with Fig. 9 indicates that the effect of including anharmonicity is minor, at least for the excited state. Most likely this is a misrepresentation, as in both cases the Q_3' dissociative mode, the potential of which creates the overall band shape, was a harmonic barrier.

The key point is that explicit inclusion of higher order operators in the vibrational Hamiltonian did not markedly effect the calculated spectrum. Again we caution that the overall band shape did not account for anharmonicity in the Q_3' dissociative mode, so that future studies may prove this conclusion false.

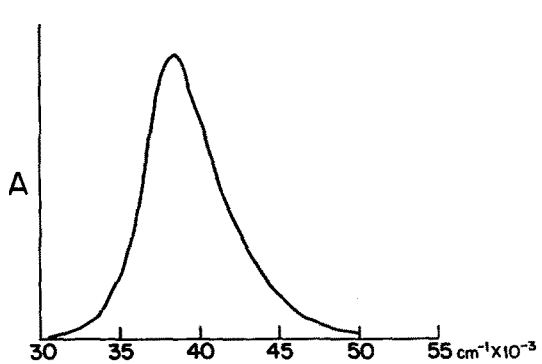

FIG. 10. As Fig. 9 except effect of anharmonicity in excited state included.

SUMMARY

In conclusion we note what has been learned from this study. A new method is employed to generate electronic spectra based solely upon *ab initio* considerations. The method directly accounts for rotational broadening and vibrational anharmonicity. Upon application to ozone, a molecule of great theoretical and practical interest, the method shows that consideration of rotational broadening and quantized vibrational levels improves the fine structure of the absorption continuum, and lends support to the contention that vibrational fine structure is possible in a purely dissociative state. Vibrational anharmonicity has been shown to have a small effect, if any, upon the overall spectrum, although this may be a spurious result.

ACKNOWLEDGMENTS

The authors thank Dr. S. M. Blinder for his helpful suggestions and the University of Michigan Computing Center for use of its facilities.

[1] Y. Tanaka, E. C. Y. Inn, and K. Watanabe, J. Chem. Phys. **21**, 1651 (1953).
[2] A. Barbe, C. Secroun, P. Jouve, A. Goldman, and D. G. Murcray, J. Mol. Spectrosc. **86**, 286 (1981).
[3] (a) A. Barbe, C. Secroun, P. Jouve, C. Camy-Peyret, and J. M. Flaud, J. Mol. Spectrosc. **75**, 103 (1979); (b) V. M. Devi, S. P. Reddy, K. N. Rao, J. M. Flaud, and C. Camy-Peyret, *ibid.* **77**, 156 (1979).
[4] A. Barbe, C. Secroun, A. Goldman, and J. R. Gillis, J. Mol. Spectrosc. **49**, 377 (1983).
[5] A. Barbe, C. Secroun, A. Goldman, and J. R. Gillis, J. Mol. Spectrosc. **49**, 171 (1974).
[6] (a) S. Carter, I. M. Mills, J. N. Murrell, and A. J. C. Varandas, Mol. Phys. **45**, 1053 (1982); (b) S. Carter, I. M. Mills, and R. N. Dixon, J. Mol. Spectrosc. **106**, 411 (1984).
[7] W. L. Feng, O. Novaro, and J. G. Prieto, Chem. Phys. Lett. **111**, 297 (1984).
[8] F. S. Johnson, J. D. Purrell, R. Tousey, and K. Watanabe, J. Geophys. Res. **57**, 157 (1952).
[9] *Ozone Chemistry and Technology* (American Chemical Society, Washington, DC, 1959).
[10] L. R. Koller, *Ultraviolet Radiation* (Wiley, New York, 1965).
[11] R. T Pack, J. Chem. Phys. **65**, 4765 (1976).
[12] G. Herzberg, *Electronic Spectra and Electronic Structure of Polyatomic Molecules* (Van Nostrand Reinhold, New York, 1966), Chaps. 4 and 5.
[13] J. W. Rabelais, J. M. McDonald, V. Scherr, and S. P. McGlynn, Chem. Rev. **71**, 73 (1971).
[14] R. D. Hudson, Rev. Geophys. Space Phys. **9**, 305 (1971).
[15] P. J. Hay and T. H. Dunning, Jr., J. Chem. Phys. **67**, 2290 (1977).
[16] K. H. Thunemann, S. D. Peyerimhoff, and R. J. Buenker, J. Mol. Spectrosc. **70**, 432 (1978).
[17] C. W. Wilson, Jr. and D. G. Hopper, J. Chem. Phys. **74**, 595 (1981).
[18] J. S. Wright, S. Shih, and R. J. Buenker, Chem. Phys. Lett. **75**, 513 (1980).
[19] J. N. Murrell, K. S. Sorbie, and A. J. C. Varandas, Mol. Phys. **32**, 1359 (1976).
[20] J. N. Murrell and S. Farantos, Mol. Phys. **34**, 1185 (1977).
[21] (a) G. D. Carney, L. A. Curtiss, and S. R. Langhoff, J. Mol. Spectrosc. **61**, 371 (1976); (b) S. M. Adler-Golden, S. R. Langhoff, C. W. Bauschlicher, Jr., and G. D. Carney, J. Chem. Phys. **83**, 255 (1985).

[22]P. J. Hay, R. T Pack, R. B. Walker, and E. J. Heller, J. Phys. Chem. **86**, 862 (1982).
[23]M. G. Sheppard and R. B. Walker, J. Chem. Phys. **78**, 7191 (1983).
[24]S. M. Adler-Golden, J. Quantum. Spectrosc. Radiat. Transfer **30**, 175 (1983).
[25]W. Kaplan, *Advanced Mathematics for Engineers* (Addison–Wesley, Reading, MA, 1981).
[26]B. T. Darling and D. M. Dennison, Phys. Rev. **57**, 128 (1940).
[27]A. Barbe, C. Secroun, P. Jouve, J. M. Flaud, and C. Camy-Peyret, J. Mol. Spectrosc. **80**, 185 (1980).
[28]D. Papousek and M. R. Aliev, *Molecular Vibrational–Rotational Spectra*; *Studies in Physics and Theoretical Chemistry* (Elsevier, Amsterdam, 1982), Vol. 17.
[29]J. K. G. Watson, J. Chem. Phys. **46**, 1935 (1967).
[30]D. Kivelson and E. B. Wilson, Jr., J. Chem. Phys. **20**, 1575 (1952).
[31]Y. Y. Kwan, J. Mol. Spectrosc. **71**, 260 (1978).
[32]E. Heilbronner, H. Günthard, and R. Gerdil, Helv. Chim. Acta **39**, 1171 (1956).
[33]A. Goldman, J. R. Gillis, D. G. Mucray, A. Barbe, and C. Secroun, J. Mol. Spectrosc. **96**, 279 (1982); also see N. Monnanteuil, J. C. Depannemaecker, J. Bellet, A. Barbe, C. Secroun, and P. Jouve, *ibid.* **71**, 399 (1978).
[34]L. L. Lohr and A. Helman, J. Comp. Chem. (in press).
[35]L. L. Lohr and J.-M. Popa, J. Chem. Phys. **84**, 4196 (1986).
[36]R. Kubo and Y. Toyozawa, Prog. Theor. Phys. **13**, 160 (1955).
[37]W. J. Ehlhardt and L. L. Lohr, J. Chem. Phys. **67**, 1935 (1977).
[38]J. W. Simons, R. J. Paur, H. A. Webster III, and E. J. Bair, J. Chem. Phys. **59**, 1203 (1973).
[39]A. Sinha, D. Imre, J. H. Goble, Jr., and J. L. Kinsey, J. Chem. Phys. **84**, 6108 (1986).